Multimorphism in molecular monolayers: Pentacene on Cu(110)

Kathrin Müller,[1] Abdelkader Kara,[2] Timur K. Kim,[3] Rolf Bertschinger,[1] Andreas Scheybal,[1] Jürg Osterwalder,[4] and Thomas A. Jung[1]

[1]*Laboratory for Micro- and Nanotechnology, Paul Scherrer Institut, CH-5232 Villigen PSI, Switzerland*

[2]*Department of Physics, University of Central Florida, Orlando, Florida 32816, USA*

[3]*Leibniz Institute for Solid State Research, IFW-Dresden, D-01171 Dresden, Germany*

[4]*Institute of Physics, University of Zürich, CH-8057 Zürich, Switzerland*

(Received 21 January 2009; revised manuscript received 1 May 2009; published 18 June 2009)

The architecture of the contacting interface between organic molecular semiconductors and metallic or insulating substrates determines its cooperative properties such as the charge injection and the charge-carrier mobility of organic thin-film devices. This paper contributes a systematic approach to reveal the evolution of the different structural phases of pentacene on Cu(110) while using the same growth conditions. Complementary measurement techniques such as scanning tunneling microscopy and low-energy electron diffraction together with *ab initio* calculations are applied to reveal the complex multiphase behavior of this system at room temperature. For coverages between 0.2 and 1 monolayer (ML) a complex multiphase behavior comprising five different phases is observed, which is associated to the interplay of molecule/molecule and molecule/substrate interactions. Multimorphism critically depends on the thermodynamics and kinetics determined by the growth parameters as well as the system itself and arises from shallow energy minima for structural rearrangements. In consequence, the multimorphism affects the interface structure and therefore the interface properties.

DOI: 10.1103/PhysRevB.79.245421 PACS number(s): 68.43.−h, 68.37.Ef, 64.75.Yz

I. INTRODUCTION

Organic semiconductors have been attracting increasing attention recently due to their application in organic electronic devices such as organic light-emitting diodes and organic field-effect transistors.[1,2] Compared to amorphous silicon, which is often used in thin-film transistors, these devices have several advantages such as low-temperature processability, low-cost fabrication, and the compatibility with a wide variety of substrates including flexible layers.[3,4] For high quality organic electronic devices, high charge-carrier mobility, and good conductivity are required. A promising organic semiconductor showing these characteristics is pentacene which shows high intrinsic charge-carrier mobility without doping.[4]

The organic/inorganic interfaces between the organic semiconductor and the gate dielectric as well as the contacting electrodes play a crucial role for the performance of organic electronic devices.[5,6] Specifically, the adsorbate/substrate interaction during the initiation of growth affects the structure of the first molecular layer and thus influences cooperative properties such as the charge injection at the metal/semiconductor interface and the charge-carrier mobility. Hence, it is an important task to understand the interaction between metallic or insulating substrates and the first layer of the adsorbate in dependence of growth parameters by studying the interface structure. For example, Thayer *et al.*[7] have reported that the orientation of adsorbed pentacene strongly depends on the electronic structure of the substrate. Pentacene molecules prefer to lie flat on metallic substrates due to their π electrons interacting with the near Fermi-level electronic states of the metal. In contrast, the molecules stand upright on insulators and semiconductors such as SiO_2,[8] organically terminated Si,[9] or Bi(001).[10]

The (110)-oriented face-centered-cubic single-crystal surfaces are particularly interesting substrates because their twofold symmetry prohibits the formation of rotational domains for adsorbates which also exhibit a twofold symmetry such as polyacenes. For example, Lukas *et al.*[11] have observed long-range self-ordering by the formation of widely spaced rows of close packed pentacene molecules on Cu(110) after annealing the pentacene covered sample to 400 K.

More recently Söhnchen *et al.*[12] and Lukas *et al.*[13] have reported the coexistence of a $p(6.5\times2)$ structure with a $c(13\times2)$ structure of a pentacene monolayer (ML) on Cu(110), by annealing the sample during evaporation to 430 K. At these temperatures the second layer formation is thermodynamically less favorable than the nucleation of a highly ordered monolayer with few defects. Pentacene layers with a similar structure have been shown by Chen *et al.*[14] For multilayers evaporated on the monolayer preassembled as described above, the molecules are tilted around the long axis by an angle of 28° with respect to the Cu(110) substrate for thicknesses below 2 nm. With increasing pentacene coverage this orientation becomes unstable and a new phase with molecules standing upright exhibiting a tilt angle of 73° develops, which is observed consistently for multilayers and thin films up to at least 50 nm thickness.[12]

The characteristically different two-dimensional (2D) arrangements observed for pentacene in the monolayer—the widely spaced rows of closed packed molecules[11] and the $p(6.5\times2)$ structure[12]—show that the phase behavior of pentacene on Cu(110) is so far not well understood. Thus, the study reported here contributes a systematic approach to reveal the growth of pentacene on Cu(110) from the nucleation at a few percents of a monolayer to the evolution of the different structural phases up to the most densely packed monolayer while using the same growth conditions. Specifi-

cally, the study reported here has been carried out at room temperature without annealing of the pentacene adlayer. Therefore, this study provides an essential basis to understand how the molecule/substrate and the intermolecular interaction affect the layer structure at this technologically relevant interface.

II. EXPERIMENTAL SECTION

The experiments were carried out in a multichamber UHV system with a base pressure of less than 5×10^{-10} mbar. Cu(110) single crystals purchased from Mateck[15] were cleaned by repeated cycles of argon-ion sputtering and subsequent annealing to 750 K. The quality and cleanliness of the single crystals were checked with x-ray photoelectron spectroscopy (XPS), low-energy electron diffraction (LEED), and scanning tunneling microscopy (STM). After the final annealing step, the samples were cooled to room temperature and then the pentacene was thermally evaporated on the samples kept at room temperature. The evaporation rate (0.2–0.5 ML/min) was controlled by a quartz crystal microbalance. For rates in this range it was found that the adsorbate structure does not depend on the deposition rate. After evaporation of the molecules, the samples were examined by STM, LEED, and XPS. STM images were recorded with an Omicron UHV-STM/AFM at ambient temperature in constant current mode using electrochemically etched and *in situ* sputtered tungsten tips.

The x-ray photoelectron spectra were used to determine the chemical composition of the organic adlayer (e.g., no oxygen contamination was found in the XPS spectra) and to quantify the molecular coverage. One ML coverage in this paper corresponds to the most densely packed monolayer we observed during our studies, i.e., the (6 −1, 1 4) layer as specified and shown below.

III. COMPUTATIONAL METHOD

A comprehensive study of energetics and electronic structure was made by solving Kohn-Sham equations[16,17] in a plane-wave basis set using the Vienna *ab initio* simulation package (VASP).[18–20] Exchange-correlation interactions are included within the generalized gradient approximation (GGA) in the Perdew-Burke-Ernzerhof form.[21] The electron-ion interaction is described by the projector augmented wave method in its implementation of Kresse and Joubert.[22,23] A plane-wave energy cutoff of 400 eV was used for all calculations and is found to be sufficient for these systems. The bulk lattice constant for Cu was found to be 3.655 Å using a *k*-point mesh of $10\times10\times10$. This value is by about 1.1% larger than the experimental one (3.615 Å), a typical trend when using GGA. The slab supercell approach with periodic boundaries is employed to model the surface and the Brillouin-zone sampling is based on the technique devised by Monkhorst and Pack.[24] The slab consists of five layers of Cu(110) each containing 14 atoms (7×2). The choice of five layers was made on the assumption that the adsorbed molecule might introduce substantial structural perturbations to the substrate, hence only the bottom layer was kept fixed as in bulk copper. In all our calculations we used a *k*-point mesh of $2\times6\times1$.

Initially, the unperturbed flat pentacene molecule was placed at about 3.5 A above the substrate at an arbitrary lateral position. A few lateral positions of the molecules have been tried as starting positions and the minimum energy was found to be the same for all configurations.

IV. RESULTS AND DISCUSSION

Figure 1(a) (bottom) shows an STM image of a sample covered with 0.5 ML of pentacene. Molecular adsorbates are rarely resolved individually due to their high mobility relative to the scanning speed of the STM tip (approx. 0.5 s/line). The characteristic lines extending along the $[1\bar{1}0]$ direction which are visible in the STM image correspond to pentacene molecules anisotropically diffusing along the grooves of the Cu(110) crystal. At step edges or kinks of the substrate individual pentacene molecules are observed in a pinned state. This shows that the pentacene diffusion generally does not proceed across the substrate steps. The pinned molecules are oriented with their long axis along the $[1\bar{1}0]$ direction, which agrees well with earlier studies of pentacene on Cu(110).[11–14] LEED data [Fig. 1(a), top left] taken on this sample covered by 0.5 ML of pentacene exhibits oval halos around the [0 0 1] spots. These ovals cross the [0 0 1] direction at 1/3 of the substrate reciprocal lattice vector which corresponds to an average distance of three Cu-lattice constants between $[1\bar{1}0]$ diffusion channels occupied with pentacene. Thus, this structure will be called a mobile $(n\times3)$ phase. The three Cu-lattice constants spacing and the direction of the highest mobility are also presented in the scheme of the adsorption structure in Fig. 1(a), top right. This mobile adlayer structure was observed for pentacene coverages up to 0.5 ML. A weak long-range ordering as well as tip induced mobility were also shown for tetracene on Cu(110).[14]

Differences in the diffusion constants depending on the relative substrate crystallographic direction and the molecular orientation were also shown for other organic molecules on the Cu(110) surface such as decacyclene and hexa-tert-butyl-decacylene,[25] azobenzene,[26] as well as the so-called "violet lander" molecule ($C_{108}H_{104}$).[27] For all these molecules no diffusion along the [0 0 1] direction has been observed, whereas they are diffusive along the $[1\bar{1}0]$ channels. Specifically, Linderoth *et al.*[26] showed that at low temperatures (120–170 K) the diffusion in the $[1\bar{1}0]$ direction for azobenzene oriented with the long axis parallel to the $[1\bar{1}0]$ direction is six times faster than for molecules oriented perpendicular to the diffusion channel. In the case of pentacene reported here, the molecules are also oriented with their long axes parallel to the $[1\bar{1}0]$ direction, which is a similar situation to the azobenzene orientation with highest diffusion. This explains the considerable diffusion along the $[1\bar{1}0]$ direction for low coverages of pentacene at room temperature.

This high degree of diffusion for low-molecular coverage shows that the diffusion barrier of an individual molecule along the $[1\bar{1}0]$ direction is rather low at room temperature.

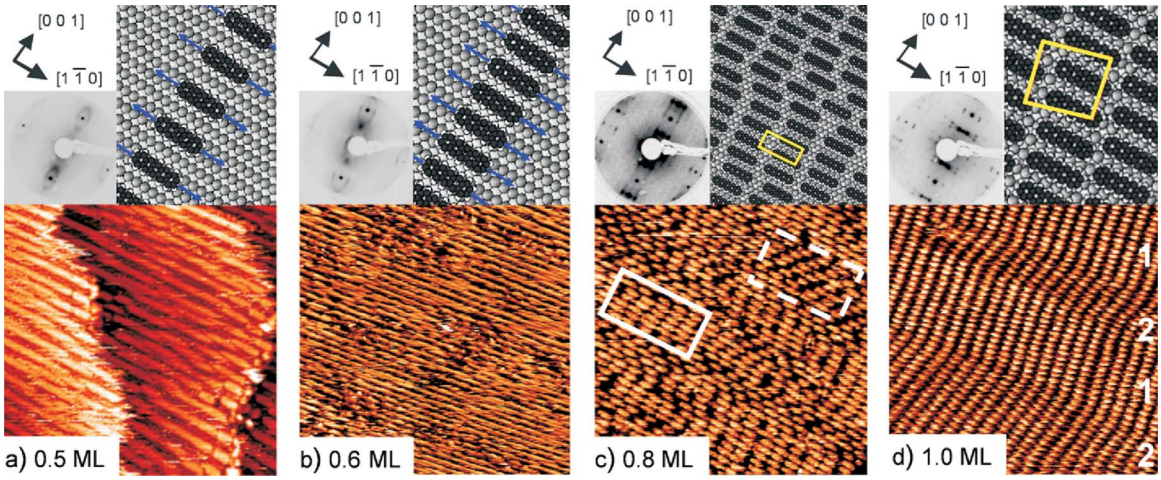

FIG. 1. (Color online) Structures of the pentacene adlayers on Cu(110). Bottom: STM images 25×25 nm^2. Top right: schemes of the adsorption structure; the scheme in (c) covers a larger area to show the degree of disorder; for clarity only one mirror domain (domain 1) is shown in scheme (d). Top left: LEED patterns at (a) and (b) 48 eV, (c) 53 eV, (d) 63 eV. (a) 0.5 ML of pentacene; STM image reveals diffusive molecules in the adatom channels and some molecules pinned at the step edges, the adsorption structure shows the three Cu-atoms distance between the neighboring diffusion channels; (b) 0.6 ML of pentacene: the diffusion channels are closer together (two Cu-atoms spacing) than in (a); (c) 0.8 ML of pentacene; the STM image shows two different adsorption structures marked with white rectangles (see discussion in the text), LEED reveals a slightly disordered (7×2) structure; (d) 1 ML of pentacene: STM image showing nicely ordered molecules in two mirror domains, indicated by the white numbers, revealing a (6 −1, 1 4) structure, each row of pentacene molecules is shifted by one Cu atom along the [0 0 1] direction.

Our calculations showed a diffusion barrier of 150 meV. Additionally, we can conclude that the interaction between the pentacene molecules adsorbed in the same $[1\bar{1}0]$ row is small and no such linear condensation is induced. The separation of the diffusion channels by three Cu-atoms spacing reduces the interaction between the molecules in the [0 0 1] direction and indicates a weak interaction between the adsorbates in neighboring diffusion channels. In contrast, C_{60} forms ordered 2D arrays also for coverages below 1 ML on noble metal surfaces[28,29] and one-dimensional arrays at step edges,[30] due to its considerable cohesive energy. For the case of pentacene on Cu(110), the interaction between the pentacene molecules after adsorption is too small to immobilize the molecules on the surface for low coverages. The existence of a higher density mobile phase (see below) leads to the conclusion that the intermolecular interaction between molecules in neighboring diffusion channels is repulsive. The mobility of the molecules in the diffusion channels of the Cu(110) substrate can be reduced by additional exposure to oxygen, which serves as pinning centers for the molecules and as nucleation sites for the condensed phase.[31]

A second mobile phase exists for coverages between 0.5 and 0.6 ML [cf. Fig. 1(b)]. Here, the LEED pattern also shows oval halos but these cross the [0 0 1] direction at $\frac{1}{2}$ of the substrate reciprocal lattice vector [cf. Fig. 1(b), top left]. This indicates that due to the higher coverage the distance between occupied diffusion channels decreases to two Cu atoms instead of three Cu atoms as shown in Fig. 1(a). Thus, this adsorption structure can be called a mobile $(n\times2)$ phase. In the STM image in Fig. 1(b) the diffusive molecules are closer together in the [0 0 1] direction than in Fig. 1(a). This is also indicated in the schematic representation of the adsorption structure (Fig. 1, top right). Additionally, few individually condensed molecules can be observed not only at defects such as step edges and kinks but also on the flat terraces indicating the onset of molecular nucleation. The fact that the occupied diffusion channels move closer together while maintaining the mobility of the molecules in the $[1\bar{1}0]$ channels indicates that the repulsive interactions between the molecules in neighboring channels are comparably low.

For coverages higher than 0.6 ML the diffusion of the pentacene molecules decreases due to the higher occupancy of the available adsorption sites and due to site blocking of nearest neighbors within the adatom rows. Consequently, single molecules are mostly resolved in the STM images [Fig. 1(c), bottom] while few still exhibit a limited mobility. The layer structure at this coverage is characterized by a distance corresponding to twice the Cu-lattice constant along the [0 0 1] direction. This observation in the STM data is also confirmed by the spots observed at $\frac{1}{2}$ of the substrate reciprocal-lattice vector in the [0 0 1] direction in the LEED pattern [Fig. 1(c), top left]. In this coverage range—0.6 to 0.8 ML—different arrangements of the molecules can be identified. On some parts of the STM image the molecules tend to form rows along the [0 0 1] direction [highlighted by the white continuous rectangle in Fig. 1(c)]; on other parts they do not show a specific ordering [highlighted by the white dashed rectangle in Fig. 1(c)]. The presence of differently arranged molecules marked in the STM image demonstrates the lack of long-range order, which is also well represented in the LEED data which exhibits diffraction stripes along the [0 0 1] direction [cf. Fig. 1(c), top left]. The six stripes in between the fundamental spots in the $[1\bar{1}0]$ direction indicate that the average distance between neighboring molecules in this direction is corresponding to seven Cu at-

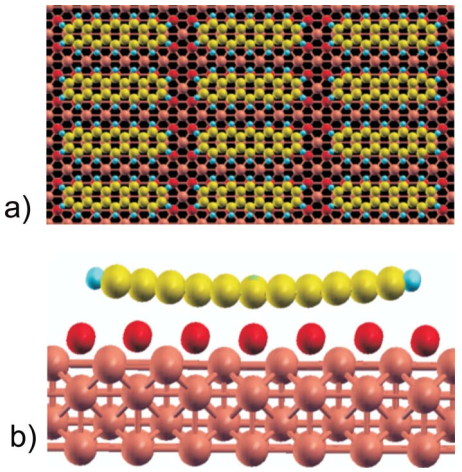

FIG. 2. (Color online) Calculation of the pentacene adsorption sites on Cu(110) for the (7×2) structure; light gray (yellow): C atoms, small and darker gray (blue): H atoms, dark gray (red): surface Cu atoms; (a) top view: C atoms of the molecule adsorb on top of the Cu atoms of the first layer; (b) side view indicating bending of the molecule by approximately 0.4 Å.

oms, therefore we call this structure a (7×2) structure despite the absence of long-range order. A sketch of the arrangement of the pentacene molecules for coverages between 0.6 and 0.8 ML is shown in the top right of Fig. 1(c).

DFT calculations for a single molecule on Cu(110) show that the pentacene molecules adsorb preferably with the C atoms on top of the Cu atoms of the first layer [cf. Fig. 2(a), the first layer atoms are colored dark gray (color online; red) for clarity]. Because of the good match between the Cu-lattice constant and the phenyl spacing in the pentacene molecules each phenyl ring is in the same position with respect to the Cu lattice. The calculations additionally show that the molecules are bent out of the surface plane by 0.4 Å; i.e., the center of the molecule is closest to the metal substrate [cf. Fig. 2(b)]. The adsorption energy was calculated to be 1.59 eV. For the slightly different (6.5×2) adsorption structure reported in Ref. 12 an adsorption energy of 2.1 eV has been determined by thermal desorption. This considerable difference probably results from the fact that our calculations have been performed for a single molecule while the adsorption energy was experimentally determined for 1 ML of pentacene, i.e., also including the intermolecular interaction. For comparison the adsorption energy of adenine on Cu(110) is calculated to 0.34 eV (Ref. 32) and the adsorption energy of NTCDA [1, 4, 5, 8-naphtalene-tetracarboxylic-dianhydride on Ag(110) and Ag(100) is 0.9 eV and 1.0 eV, respectively].[33] This shows that the molecules interact more strongly with the Cu substrate than in the case of weakly physisorbed systems. An additional indication for the strong molecule/substrate interaction is that all molecules seem to lie flat on the Cu(110) surface while it has been reported that a mixed layer of flat lying and tilted (by 90° around the long axis) molecules can be observed for pentacene on Au(110).[34] This strong interaction between the molecules and the substrate is also observed in angle-resolved photoelectron spectroscopy measurements of pentacene on Cu(110).[35,36] The calculated bending of the molecules is also consistent with

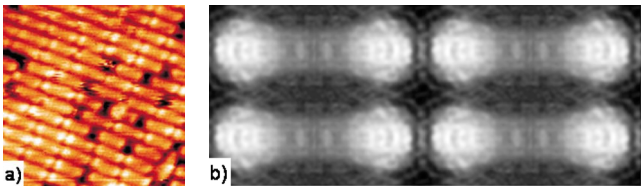

FIG. 3. (Color online) (a) 0.7 ML pentacene on Cu(110): STM image 8×8 nm^2 indicating the bending of the pentacene molecules by the white ends of the molecules; (b) calculated STM image.

the STM data shown in Fig. 3(a) where the ends of the molecules are imaged brighter than the centers; an observation which fits well with the calculated STM image in Fig. 3(b).

The (7×2) structure reported here shows a slightly lower packing density compared to the previously reported $p(6.5\times2)$ structure.[12] The small difference in the packing density along the $[1\bar{1}0]$ direction (6.5 vs 7 Cu atoms) and the lower degree of long-range ordering of the (7×2) structure is attributed to the slightly smaller coverage of our samples and to the different parameters used during sample preparation. From the described observations it is plausible that a number of $(z\times2)$ phases [z=6,[14] 6.5,[12] and 7 (this work)] can be prepared due to the expected small energy difference between such phases and in dependence of preparation parameters such as coverage, annealing temperature, and evaporation rate. Different annealing temperatures and evaporation rates lead to a change in the mobility of the molecules, which consequently may change the spacing of the molecules in the $[1\bar{1}0]$ direction. We have to point out that the distance of seven Cu atoms is an average and the molecular separation is varying around six to eight Cu atoms in our data.

Coverage of a full monolayer leads to a characteristically different highly ordered structure with very few defects. The molecules are oriented in rows which are tilted by $\pm9°$ out of the [0 0 1] direction leading to two mirror domains, while maintaining the molecular orientation of the long axis parallel to the $[1\bar{1}0]$ direction [cf. Fig. 1(d)]. The neighboring pentacene rows are shifted by one Cu atom along the [0 0 1] direction, which results in an oblique unit cell. The LEED pattern shows discrete spots forming rows, which are tilted out of the $[1\bar{1}0]$ direction [cf. Fig. 1(d), top left]. This observation, together with the molecular resolution STM data, suggests an adsorption structure like the one shown in Fig. 1(d), top right, which can be described by a (6 −1, 1 4) matrix, each unit cell containing two molecules. Occasionally, but on comparably smaller surface areas a coexisting phase was observed. Here the neighboring molecular rows are not shifted with respect to the Cu substrate leading to aligned molecules with respect to the short axis of the molecules (cf. Fig. 4, in between the white lines of the STM image). This structure, which has the same packing density as the (6 −1, 1 4) structure can be described by a (6.25 −1, 0 4) matrix.

These two structures, which we observed for 1 ML coverage, exhibit a slightly higher packing density than the previously reported $p(6.5\times2)$ and $c(13\times2)$ phases.[12,13] Note that the packing density for the (6 −1, 1 4) structure is

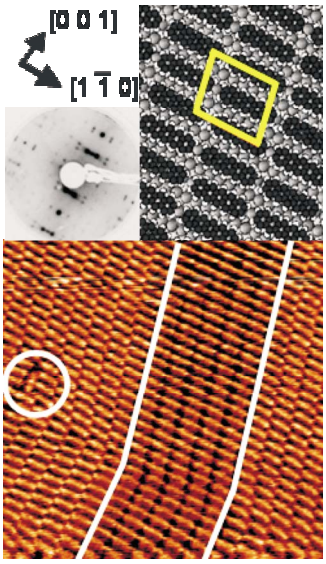

FIG. 4. (Color online) 1 ML of pentacene. Bottom: STM image 20×20 nm^2; top left: LEED pattern at 63 eV. Top right: scheme of the adsorption structure; in between the white lines of the STM image an area of molecular rows not shifted along the [0 0 1] direction is visible which can be described by a (6.25 −1, 0 4) matrix.

0.87 molecules/nm^2, while the packing density of the $p(6.5\times2)$ phase is 0.83 molecules/nm^2. Beside this small difference in the packing density, the main difference between the structures is the tilt of the molecular rows out of the [0 0 1] direction, which is clearly visible in the STM image and in the LEED pattern shown in Figs. 1(d) and 4. Additionally, it has to be emphasized that the $p(6.5\times2)$ and the $c(13\times2)$ structures were obtained by annealing of the sample at 430 K during pentacene deposition, while our sample preparation was performed at room temperature. Noteworthy, Chen *et al.*[14] mentioned that the intermolecular rows are slightly diverted away from the [0 0 1] direction due to interdigitation of the CH bonds.

Additionally, in Fig. 4 one defect consisting of a molecule oriented perpendicular to the $[1\bar{1}0]$ direction can be seen (white circle). Due to the high packing density this molecule is sterically hindered to rotate back into the preferred orientation, which is along the $[1\bar{1}0]$ direction. These defect sites, however, are very rarely observed in the STM images. This fact emphasizes the high quality of the self-assembled molecular layer.

Diffusing adatoms can influence the orientation of molecular adsorbates as it was shown for benzoate species on Cu substrates.[37] On the other hand it has been demonstrated that porphyrine adsorbates can change the surface reconstruction of a Au(110) surface.[38] Even weakly physisorbed glycine induces a reconstruction of the Au(110) surface.[39] Since the diffusion barrier along the channels is comparable for Au(110) (0.28 eV)[40] and Cu(110) (0.24 eV),[41] it is also important to briefly discuss the influence of the Cu adatom diffusion on the pentacene diffusion and adsorption structures shown in this paper. The diffusion barrier of pentacene along the $[1\bar{1}0]$ direction is slightly smaller (0.15 eV) than the diffusion barrier of the Cu adatoms, but still both—Cu adatoms and pentacene molecules—show a considerable diffusion along the $[1\bar{1}0]$ channels at room temperature. It is difficult to determine how exactly the diffusion of the metal adatoms influences the diffusion of the molecules and vice versa. The investigation of this complicate interaction would require additional temperature-dependent studies combined with *ab initio* calculations, which would lead far beyond the scope of this paper. However, both diffusing species compete for the same space in the channels. In our data, the horizontal streaks near the left step in the STM image in Fig. 1(a) indicate that there is considerable Cu diffusion even after adsorption of pentacene. At higher molecular coverages, after the molecular diffusion has been blocked by the occupancy of neighboring sites, the steps and kinks appear much sharper. This is consistent with the expectation that the Cu adatom diffusion is reduced at higher pentacene coverages.

On the other hand, there is no evidence for the formation of a pentacene-induced surface reconstruction as observed for pentacene on Au(110) (Refs. 42 and 43): (i) the STM data and the models presented in Figs. 1 and 4 agree well and do not indicate a modification of the surface reconstruction. (ii) The Cu(110) Shockley surface state is still present after adsorption of 1 ML of pentacene.[35] This observation excludes considerable surface reconstruction, which would probably lead to a quenching of the surface state.

For all coverages between 0.6 and 1 ML, where the mobility of the molecules is sufficiently reduced to determine the layer structure by STM and LEED studies, the growth of pentacene is commensurate with the Cu(110) lattice in both directions. For the adsorption of 1 ML of pentacene the adsorption sites differ in their relative position with respect to the $[1\bar{1}0]$ direction. Specifically, four different adsorption sites shifted by 1/4 of a Cu-lattice spacing in the $[1\bar{1}0]$ direction exist for the (6.25 −1, 0 4) structure. In contrast this shift is inexistent for the (7×2) structure as shown in the STM image in Fig. 1(c) and in the calculations in Fig. 2. Notably, at lower coverages up to 0.6 ML LEED and STM indicate commensurability along [0 0 1] direction and diffusivity along $[1\bar{1}0]$ direction.

V. CONCLUSIONS

In conclusion, we have shown five different adsorption structures of pentacene on Cu(110) to occur after deposition at room temperature (295 K) without annealing. By the comprehensive STM and LEED studies and by comparison to *ab initio* calculations, we have demonstrated that the substrate/molecular interaction is stronger than the intermolecular interaction leading to a complex multiphase behavior. The different stages of this phase behavior before nucleation of the second layer are characterized by molecular mobility, molecular bending, their structure modified, e.g., by their relative position of neighboring molecules and different packing densities of the linear pentacene molecules.

McCrone[44] stated for the crystal structures of organic molecules, that "every compound has different polymorphic forms, and that, in general, the number of forms known for a

given compound is proportional to the time and money spent in research on that compound." We realized the same for the 2D adsorption polymorph of pentacene on Cu(110): although a lot has already been published about this system, we have shown two diffusive adsorbate phases and three different condensed phases to occur at different coverages but with the same preparation parameters. The latter helped to refine already mentioned adsorbate structures.

The observation of five distinctively different adlayer phases in the monolayer for the comparably simple shape and adsorption geometry of the pentacene on Cu(110) system suggests that the phase behavior may be even more featured for more complex molecular adsorbates. Complex phase evolutions like in the demonstrated case will only be revealed by detailed studies—using complementary techniques—of the molecular packing with consistent parameter sets in a wide coverage range. The fact that the molecular packing and orientation at the interface influences any cooperative behavior such as charge injection, charge-carrier mobility, and the emergence of intermolecular and interface electronic states motivates the detailed comparison of experiment and theory also for other interfaces relevant for organic electronics. The fabrication of specific organic/inorganic interfaces by controlling the first layer growth may offer a way to control the cooperative electronic and optoelectronic behavior of such interfaces, also within devices.

Note added in proof. J. Martínez-Blanco *et al.* have reported three stages of the phase behavior described here, i.e., one mobile phase and two condensed phases for different coverages of pentacene on Cu(110).[45]

ACKNOWLEDGMENTS

Funding by the Swiss National Science Foundation, the NCCR on Nanoscale Science, and the Paul Scherrer Institute were of key importance for this work. Thomas Greber and Charles Campbell are acknowledged for fruitful discussions. A.K. thanks the University of Zurich for support; his work was also partially supported by a UCF start-up fund. The following persons gave valuable assistance and advice, thereby making this work feasible: R. Schelldorfer, D. Chylarecka, N. Ballav, J. Girovsky, N. Kappeler, and G. Günzburger.

[1] G. Horowitz, Adv. Mater. **10**, 365 (1998).
[2] B. Crone, A. Dodabalapur, Y.-Y. Lin, R. W. Filas, Z. Bao, A. LaDuca, R. Sarpeshkar, H. E. Katz, and W. Li, Nature (London) **403**, 521 (2000).
[3] G. H. Gelinck, H. E. A. Huitema, E. van Veenendaal, E. Cantatore, L. Schrijnemakers, J. B. P. H. van der Putten, T. C. T. Geuns, M. Beenhakkers, J. B. Giesbers, B.-H. Huisman, E. J. Meijer, E. M. Benito, F. J. Touwslager, A. W. Marsman, B. J. E. van Rens, and D. M. de Leeuw, Nature Mater. **3**, 106 (2004).
[4] M. Daraktchiev, A. von Mühlenen, F. Nüesch, M. Schaer, M. Brinkmann, M.-N. Bussac, and L. Zuppiroli, New J. Phys. **7**, 133 (2005).
[5] S. Y. Yang, K. Shin, and C. C. Park, Adv. Funct. Mater. **15**, 1806 (2005).
[6] S. F. Alvarado, L. Rossim, P. Müller, and W. Rieß, Synth. Met. **122**, 73 (2001).
[7] G. E. Thayer, J. T. Sadowski, F. Meyer zu Heringdorf, T. Sakurai, and R. M. Tromp, Phys. Rev. Lett. **95**, 256106 (2005).
[8] R. Ruiz, B. Nickel, N. Koch, L. C. Feldman, R. F. Haglund, A. Kahn, and G. Soles, Phys. Rev. B **67**, 125406 (2003).
[9] F.-J. Meyer zu Heringdorf, M. C. Reuter, and R. M. Tromp, Nature (London) **412**, 517 (2001).
[10] J. T. Sadowski, T. Nagao, S. Yaginuma, Y. Fujikawa, A. Al-Mahboob, K. Nakajima, T. Sakurai, G. E. Thayer, and R. M. Tromp, Appl. Phys. Lett. **86**, 073109 (2005).
[11] S. Lukas, G. Witte, and Ch. Wöll, Phys. Rev. Lett. **88**, 028301 (2001).
[12] S. Söhnchen, S. Lukas, and G. Witte, J. Chem. Phys. **121**, 525 (2004).
[13] S. Lukas, S. Söhnchen, G. Witte, and C. Wöll, ChemPhysChem **5**, 266 (2004).
[14] Q. Chen, A. J. McDowall, and N. V. Richardson, Langmuir **19**, 10164 (2003).
[15] http://www.mateck.de
[16] P. Hohenberg and W. Kohn, Phys. Rev. **136**, B864 (1964).
[17] W. Kohn and L. J. Sham, Phys. Rev. **140**, A1133 (1965).
[18] G. Kresse and J. Furthmuller, Phys. Rev. B **54**, 11169 (1996).
[19] G. Kresse and J. Furthmuller, Comput. Mater. Sci. **6**, 15 (1996).
[20] G. Kresse and J. Hafner, Phys. Rev. B **47**, 558 (1993).
[21] J. P. Perdew, K. Burke, and M. Ernzerhof, Phys. Rev. Lett. **77**, 3865 (1996).
[22] G. Kresse and D. Joubert, Phys. Rev. B **59**, 1758 (1999).
[23] P. E. Blochl, Phys. Rev. B **50**, 17953 (1994).
[24] H. J. Monkhorst and J. D. Pack, Phys. Rev. B **13**, 5188 (1976).
[25] M. Schunack, T. R. Lindetroth, F. Rose, E. Lægsgaard, I. Stensgaard, and F. Besenbacher, Phys. Rev. Lett. **88**, 156102 (2002).
[26] J. A. Miwa, S. Weigelt, H. Gersen, F. Besenbacher, F. Rosei, and T. R. Linderoth, J. Am. Chem. Soc. **128**, 3164 (2006).
[27] R. Otero, F. Hümmelink, F. Sato, S. B. Legoas, P. Thorstrup, E. Lægsgaard, I. Stensgaard, D. S. Galvão, and F. Besenbacher, Nature Mater. **3**, 779 (2004).
[28] G. Costantini, S. Rusponi, E. Giudice, C. Boragno, and U. Valbusa, Carbon **37**, 727 (1999).
[29] W. W. Pai, C.-L. Hsu, M. C. Lin, K. C. Lin, and T. B. Tang, Phys. Rev. B **69**, 125405 (2004).
[30] M. T. Cuberes, R. R. Schlittler, and J. K. Gimzewski, Appl. Phys. Lett. **69**, 3016 (1996).
[31] K. Müller, A. Kader, J. Osterwalder, and T. A. Jung (unpublished).
[32] W. G. Schmidt, K. Seino, M. Preuss, A. Hermann, F. Ortmann, and F. Bechstedt, Appl. Phys. A **85**, 387 (2006).
[33] A. Alkauskas, A. Baratoff, and C. Bruder, Phys. Rev. B **73**, 165408 (2006).
[34] G. Bavdek, A. Cossaro, D. Cvetko, C. Africh, C. Blasetti, F. Esch, A. Morgante, and L. Floreano, Langmuir **24**, 767 (2008).
[35] A. Scheybal, K. Müller, R. Bertschinger, M. Wahl, A. Ben-

dounan, P. Aebi, and T. A. Jung, Phys. Rev. B **79**, 115406 (2009).
[36] H. Yamane, D. Yoshimura, E. Kawabe, R. Sumii, K. Kanai, Y. Ouchi, N. Ueno, and K. Seki, Phys. Rev. B **76**, 165436 (2007).
[37] C. C. Perry, S. Haq, B. G. Frederick, and N. V. Richardson, Surf. Sci. **409**, 512 (1998).
[38] T. A. Jung, R. R. Schlittler, and J. L. Gimzewski, Nature (London) **386**, 696 (1997).
[39] X. Zhao, H. Yan, R. G. Zhao, and W. S. Yang, Langmuir **18**, 3910 (2002).
[40] F. Montalenti and R. Ferrando, Surf. Sci. **433-435**, 445 (1999).
[41] M. Karimi, T. Tomkowski, G. Bidali, and O. Biham, Phys. Rev. B **52**, 5364 (1995).
[42] Ph. Guaino, D. Carty, G. Hughe, O. McDonald, and A. A. Cafolla, Appl. Phys. Lett. **85**, 2777 (2004).
[43] F. Evangelista, A. Ruocco, D. Pasca, C. Baldacchini, M. G. Betti, V. Corradini, and C. Mariani, Surf. Sci. **566-568**, 79 (2004).
[44] W. C. McCrone, in *Polymorphism in Physics and Chemistry of the Organic Solid-State*, edited by D. Fox, M. M. Labes, and A. Weisemberg (Interscience, New York, 1965), p. 726.
[45] J. Martínez-Blanco, M. Ruiz-Osés, V. Joco, D. I. Sayago, P. Segovia, and E. G. Michel, J. Vac. Sci. Technol. B **27**, 863 (2009).